JCI The Journal of Clinical Investigation

Fatty acid transport protein-2 inhibition enhances glucose tolerance through α-cell-mediated GLP-1 secretion

Shenaz Khan, … , Domenico Accili, Jeffrey R. Schelling

J Clin Invest. 2025. https://doi.org/10.1172/JCI192011.

Research In-Press Preview Endocrinology Metabolism

Graphical abstract

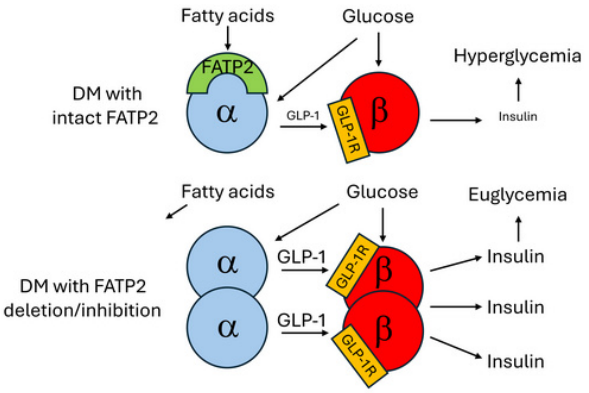

Fatty acid transport protein-2 inhibition enhances glucose tolerance through α-cell-mediated GLP-1 secretion

Shenaz Khan[1], Robert J. Gaivin[1], Zhiyu Liu[1], Vincent Li[1], Ivy Samuels[2], Jinsook Son[3], Patrick Osei-Owusu[1], Jeffrey L. Garvin[1], Domenico Accili[3], Jeffrey R. Schelling[1,4]

1. Department of Physiology & Biophysics, Case Western Reserve University School of Medicine, Cleveland, OH
2. Louis Stokes Cleveland VA Medical Center, VA Northeast Ohio Healthcare System; Department of Ophthalmic Research, Cole Eye Institute, Cleveland, OH
3. Department of Medicine and Naomi Berrie Diabetes Center, Vagelos College of Physicians and Surgeons of Columbia University, New York, NY
4. Department of Medicine, Case Western Reserve University School of Medicine, Cleveland, OH

COI: The authors have declared that no conflict of interest exists.

Correspondence: Jeffrey R. Schelling, MD
Department of Physiology & Biophysics
School of Medicine
Case Western Reserve University
10900 Euclid Avenue
Robbins Building, E515
Cleveland, OH 44106
Phone: 216-368-0076
email: jrs15@case.edu

ABSTRACT

Type 2 diabetes affects more than 38 million people in the US, and a major complication is kidney disease. During the analysis of lipotoxicity in diabetic kidney disease, global fatty acid transport protein-2 (FATP2) gene deletion was noted to markedly reduce plasma glucose in db/db mice due to sustained insulin secretion. To identify the mechanism, we observed that islet FATP2 expression was restricted to α-cells, and α-cell FATP2 was functional. Basal glucagon and alanine-stimulated gluconeogenesis were reduced in FATP2KO db/db compared to db/db mice. Direct evidence of FATP2KO-induced α-cell-mediated glucagon-like peptide-1 (GLP-1) secretion included increased GLP-1-positive α-cell mass in FATP2KO db/db mice, small molecule FATP2 inhibitor enhancement of GLP-1 secretion in αTC1-6 cells and human islets, and exendin[9-39]-inhibitable insulin secretion in FATP2 inhibitor-treated human islets. FATP2-dependent enteroendocrine GLP-1 secretion was excluded by demonstration of similar glucose tolerance and plasma GLP-1 concentrations in db/db FATP2KO mice following oral versus intraperitoneal glucose loading, non-overlapping FATP2 and preproglucagon mRNA expression, and lack of FATP2/GLP-1 co-immunolocalization in intestine. We conclude that FATP2 deletion or inhibition exerts glucose-lowering effects through α-cell-mediated GLP-1 secretion and paracrine β-cell insulin release.

INTRODUCTION

Type 2 diabetes affects more than 38 million people in the US (830 million worldwide) and is a major public health problem due to morbidity and mortality from microvascular (kidney disease, retinopathy, neuropathy) and macrovascular (myocardial infarction, stroke, peripheral vascular) complications. The pathophysiologic mechanisms are complex, with substantial contributions from altered glucose and lipid metabolism (1, 2).

The lipid abnormalities in diabetes include increased plasma fatty acid concentrations (3). Fatty acids circulate predominantly as non-covalently bound complexes with albumin or as covalently-linked esters with glycerol to form triglycerides. Cellular fatty acid uptake is facilitated by a family of six evolutionarily conserved plasma membrane fatty acid transport proteins (FATP1-6), which are expressed in a tissue-specific fashion (4).

FATP2 is a major fatty acid transporter in liver and kidney, and has been implicated in the pathophysiology of metabolic dysfunction-associated steatotic liver disease (MASLD) and diabetic kidney disease (5). Modest reduction of fasting plasma glucose was observed in mice with liver-specific FATP2 gene (*Slc27a2*) deletion (6). Inhibition of FATP2 by shRNA tail vein injection in high fat diet-induced diabetic mice also resulted in mild plasma glucose reduction, as well as improved insulin sensitivity (7). Because tail vein-injected siRNA uptake is primarily by liver (8), it was assumed that the hypoglycemic effect of FATP2 inhibition was mediated by enhanced hepatic glucose metabolism. However, tail vein-injected reporter siRNAs are detectable in other FATP2-expressing organs, including intestine and pancreas (9, 10), which raises the possibility that extrahepatic FATP2 inhibition contributes to the glucose-lowering phenotype.

In contrast to the modest glucose reduction with liver FATP2 inhibition (6, 7), global FATP2 deletion was associated with profoundly lower plasma glucose in genetic and inducible mouse models of type 2 diabetes (11). Furthermore, diabetic mice with intact FATP2 developed reduced plasma insulin, whereas diabetic mice with FATP2 deletion demonstrated islet hypertrophy and sustained hyperinsulinemia (11). These observations suggest that FATP2 inhibition enhances pancreatic β-cell mass and function. Localization of FATP2 to specific pancreatic cells, and assignment of FATP2 inhibition to pancreatic endocrine functions, have not been previously described.

Glucose-stimulated insulin secretion (GSIS) is augmented by glucagon-like peptide (GLP)-1 in diabetes (12). Following a glucose- or fat-containing meal, GLP-1 is secreted into the circulation by enteroendocrine L-cells in the distal ileum and proximal colon, and ultimately binds to GLP-1 receptors on pancreatic β-cells to stimulate insulin secretion (13). Fatty acids can also directly stimulate GSIS through binding to free fatty acid receptor 1 (FFAR1), which is expressed at low levels on β-cells (14, 15). The insulinotropic effects of fatty acids in acute models are counterbalanced by chronic fatty acid-induced α- and/or β-cell desensitization and decreased insulin secretion (16), which may be mediated by specific fatty acid receptors.

Pancreatic α-cells also secrete GLP-1, which enhances GSIS through paracrine activation of the β-cell GLP-1 receptor (12, 15, 17), particularly under conditions of β-cell stress (18). The primacy of paracrine GLP-1 is supported by observations that GLP-1 secreted by enteroendocrine cells has a half-life of only two minutes (19), due to proteolysis by local dipeptidyl peptidase (DPP)-4. It has therefore been postulated that gut-derived GLP-1 may not achieve sufficient concentration to stimulate distant β-cell GLP-1 receptors, and an α-cell,

118 rather than enteroendocrine source of GLP-1, regulates insulin secretion under diabetic
119 conditions (18).
120 With the emergence of GLP-1 receptor agonists as weight loss drugs, there is intense
121 recent interest regarding GLP-1 regulation of lipid metabolism. However, the effect of fatty
122 acids on GLP-1 biology is much less well understood, and the influence of FATP2 inhibition on
123 GLP-1 pathways has not been investigated. In this report we describe the mechanisms of
124 insulinotropic activity by FATP2 inhibition, through augmentation of α-cell-mediated GLP-1
125 secretion.

RESULTS

Diabetic mice with global FATP2 gene deletion (FATP2KO) developed markedly reduced fasting plasma glucose (11). FATP2 is most abundantly expressed in kidney, and within kidney, exclusively in the apical proximal tubule membrane (20, 21). The proximal tubule contributes to gluconeogenesis, particularly in the pathogenesis of diabetes (22). However, deletion of proximal tubule FATP2 (Supplemental Figure 1) in an inducible model of diabetes did not alter fasting plasma glucose concentrations (Supplemental Figure 2). These data suggest that the glucose-lowering effect in global FATP2KO mice is not due to proximal tubule FATP2 gene deletion, but rather by an extrarenal mechanism.

Pancreatic islet FATP2 protein expression is upregulated in the setting of elevated glucose concentration (23), and global FATP2 gene deletion in diabetic mice was associated with increased islet area and sustained plasma insulin (11), suggesting that inhibition of FATP2 mediates protection of pancreatic islet function. Compared to diabetic *Lepr*$^{db/db}$ (db/db) mice with intact FATP2, FATP2KO db/db mice demonstrated islet hypertrophy (Figures 1A and 1B, respectively) and increased β-cell mass (Figure 1C). These data are consistent with FATP2 deletion causing rescue of β-cell failure in db/db mice (11, 24).

FATP2 mRNA is expressed in pancreas (11), and variably in α- and β-cells from scRNAseq databases (25-30). Figure 2 demonstrates that FATP2 protein co-localized exclusively with α-, but not β- or δ-cells in mice. Figure 3A demonstrates similar co-localization of FATP2 with α-cells in human pancreas, and is consistent with correlation between FATP2 and GCG (preproglucagon gene encoding glucagon and GLP-1) mRNA expression (Figure 3B). FATP2 mRNA is expressed in mouse and human pancreas tissue and α-cells (Figures 4A and 4B), but is

148 undetectable in INS-1 β-cells (not shown). Mouse pancreas and αTC1-6 cells predominantly
149 express the Fatp2a variant (Supplemental Figure 3), which contains acyl CoA synthetase activity
150 within the cytosolic domain (31), and in a plasma membrane distribution (Supplemental Figure
151 4). FATP2 mRNA expression was increased in islets from db/db compared to wild-type mice,
152 though the difference was not significant (Supplemental Figure 5). To determine whether α-cell
153 FATP2 is functional, long-chain fatty acid transport was measured in αTC1-6 cells. Fatty acid
154 uptake was blocked by the FATP2 inhibitor, Lipofermata (Figure 4C). The IC_{50} value (5.4 μM) is in
155 agreement with other epithelial cells (32, 33). The conclusion from these experiments is that α-
156 cells express functional FATP2, which is sustained with diabetes.
157 We next focused on the mechanism by which α-cell FATP2 deletion regulates insulin
158 secretion. GLP-1 and glucagon bind with high and low affinity, respectively, to the GLP-1
159 receptor on the β-cell, which facilitates GSIS (12). Random (non-fasting) plasma glucagon levels
160 were increased in db/db mice with intact FATP2, decreased in FATP2KO db/db mice, and not
161 significantly different compared to wild-type (Figure 5A), suggesting that glucagon is not the
162 stimulus for sustained insulin secretion in FATP2KO db/db mice. To address the effects of FATP2
163 deletion on glucagon-induced hepatic gluconeogenesis, alanine tolerance tests were conducted
164 in fasted db/db versus FATP2KO db/db mice. Figure 5B demonstrates transient alanine-
165 stimulated glucose increases in wild-type and FATP2 KO db/db mice, whereas db/db mice
166 experienced sustained hyperglycemia (>600 mg/dl) from 30 to 120 minutes. The data suggest
167 that the relatively modest effect on glucose in FATP2KO db/db mice reflects reduced glucagon-
168 stimulated gluconeogenesis.

We focused next on the effect of FATP2 gene deletion on GLP-1. The relative contribution of enteroendocrine L-cell- versus α-cell-derived GLP-1 on β-cell insulin secretion has been debated (34). To investigate whether enteroendocrine cells are the GLP-1 source in FATP2KO db/db mice, OGTT and IPGTT were conducted in db/db mice with or without FATP2 gene deletion. The rationale is if the major GLP-1 source is enteroendocrine, oral glucose would stimulate a greater increase in plasma GLP-1 and superior glucose tolerance compared to IP glucose (35). Four-month-old db/db and FATP2KO db/db mice were obese, though baseline weights (45 ± 9 g and 54 ± 10 g, respectively), were similar ($P > 0.05$). Figure 6A shows markedly lower fasting plasma glucose concentrations in FATP2KO db/db compared to db/db mice, consistent with previous reports (11). Plasma glucose values were >600 mg/dL in all db/db mice during OGTT and IPGTT at 30-120 min. Figures 6A and 6B show no difference between OGTT and IPGTT in FATP2KO db/db mice. Glucose disposal was also similar following OGTT vs. IPGTT in non-diabetic FATP2KO mice (Supplemental Figure 6). Importantly, plasma GLP-1 increases were similar in FATP2KO db/db mice after oral and IP glucose loading (Figure 6C). The lack of enhanced glucose tolerance and GLP-1 concentration with oral glucose suggest that α-cells, rather than enteroendocrine L-cells, are the source of GLP-1 in mice with global FATP2 gene deletion.

To further address the possibility of FATP2 effects on enteroendocrine GLP-1 secretion, FATP2 and GCG mRNA expression was evaluated in intestine segments by qPCR. Both transcripts were detected throughout the mouse GI tract, but with distinct patterns, and minimal overlap (Figure 7A and 7B). Protein expression in human distal ileum (Figure 7C and 7D) and duodenum (Figure 7E and 7F) demonstrated no FATP2/GLP-1 co-localization. Taken

191 together, the data suggest that FATP2 deletion does not directly influence GLP-1 synthesis or
192 secretion by enteroendocrine cells.

193 The next set of experiments tested the direct effects of FATP2 inhibition on α-cell GLP-1
194 secretion. Both α-cell mass and % of GLP-1-positive α-cells were increased in FATP2KO db/db
195 islets (Supplemental Figure 7). Consequently, the product of α-cell mass and % of GLP-1-
196 positive α-cells (GLP-1-positive α-cell mass) was markedly greater in FATP2KO db/db compared
197 to db/db mice (Figure 8A). FATP2 inhibition in human islets enhanced glucose-stimulated GLP-1
198 secretion, particularly under high glucose conditions (Figure 8B). Prolonged high glucose plus
199 palmitate has previously been shown to inhibit GLP-1 secretion, due to glucolipotoxicity (36). To
200 assess whether FATP2 inhibition preserves GLP-1 secretion, glucose-stimulated GLP-1 release
201 was tested in αTC1-6 cells (37, 38), in response to palmitate with or without Lipofermata pre-
202 incubation (32, 33). Figure 8C demonstrates that under low and high glucose conditions,
203 palmitate decreased αTC1-6 cell GLP-1 secretion, which was rescued by Lipofermata pre-
204 incubation. Taken together, the data indicate that FATP2 inhibition or deletion preserves α-cell
205 GLP-1 secretion.

206 Regulation of GLP-1 and glucagon expression is primarily post-transcriptional, with
207 differential cleavage of proglucagon by PC1/3 (encoded by proprotein convertase
208 subtilisin/kexin type 1, PCSK1) generating GLP-1, and by PC2 (encoded by PCSK2) to produce
209 glucagon. Adult α-cells express scant PC1/3 and secrete very little basal GLP-1, but in vivo
210 stresses, such as diabetes and aging cause α-cell hyperplasia and shift from PC2 to PC1/3
211 expression (39-42). Inhibition of FATP2 was associated with increased expression of *Pcsk1* and
212 increased ratio of *Pcsk1:Pcsk2* mRNA in mouse αTC1-6 cells (Figure 8D).

213 To investigate whether FATP2 inhibition regulates α-cell GLP-1-dependent insulin
214 secretion, GSIS was examined in human islets pretreated with palmitate, Lipofermata and/or
215 the GLP-1 receptor inhibitor exendin[9-39]. Figure 8E demonstrates that Lipofermata enhanced
216 insulin secretion (particularly under high glucose concentration conditions). Importantly, a large
217 proportion of the increase was exendin[9-39]-inhibitable, indicating that FATP2 inhibition
218 enhanced α-cell secretion of GLP-1, which acts in a paracrine manner to enhance GSIS.

DISCUSSION

Type 2 diabetes is characterized by initial hyperinsulinemia, and subsequent β-cell dedifferentiation and insulin deficiency (43). We previously showed that global FATP2 deletion in genetic and inducible mouse models of type 2 diabetes was associated with markedly decreased plasma glucose and increased plasma insulin (11). Using in vivo, ex vivo and in vitro models, we now show that the mechanism of sustained hyperinsulinemia in the setting of FATP2 inhibition or deletion is α-cell-mediated GLP-1 secretion, with paracrine stimulation of β-cell insulin secretion (graphical abstract).

The conventional dogma is that intestinal L-cells are the major source of GLP-1, which exerts potent insulinotropic effects. This mechanism has been questioned, though, due to the short half-life, and potentially insufficient GLP-1 concentration to stimulate GLP-1 receptors on distant β-cells. Additionally, deletion of α-cell *Pcsk1*, which encodes the enzyme that catalyzes the cleavage of proglucagon to GLP-1, worsens (39), and overexpression improves glucose tolerance (44). We provide substantial evidence against an enteroendocrine source of GLP-1 as the mechanism for increased plasma insulin in FATP2KO mice, including (a) no difference between plasma GLP-1 or glucose tolerance in db/db FATP2KO mice following oral vs. i.p. glucose loading, (b) non-overlapping FATP2 and GCG mRNA expression in intestine, and (c) lack of FATP2 and GLP-1 protein co-localization in intestinal cells. Additional evidence against FATP2KO regulation of enteroendocrine GLP-1 is the lack of weight loss in diabetic FATP2KO mice. The mechanism of GLP-1-mediated weight reduction is complex, but at least partly involves gut-derived GLP-1 stimulation of the vagus nerve, which leads to anorexia and delayed gastric emptying (45). FATP2KO db/db mice were slightly heavier than db/db mice, which

mitigates against an enteroendocrine GLP-1 mechanism. Furthermore, the lack of weight loss in FATP2KO db/db mice was accompanied by no difference in food intake (11), which argues against a FATPKO effect on GLP-1-mediated satiety through stimulation of hypothalamic POMC neurons. However, db/db mice harbor a leptin receptor mutation, which causes hyperphagia, and may confound interpretation of GLP-1-regulated satiety and feeding behavior in this mouse model.

Direct evidence to support α-cell-mediated GLP-1 secretion as the mechanism of FATP2KO-associated hyperinsulinemia included (a) co-localization of FATP2 with human and mouse islet α-, but not β- cells, (b) FATP2 mRNA expression in human and mouse α-, but not β-cells, (c) inhibition of fatty acid uptake by FATP2 inhibitors in α-cells, (d) increased GLP-1-positive α-cell mass in FATP2KO db/db mice, (e) increased *Pcsk1*:*Pcsk2* mRNA ratio in αTC1-6 cells treated with Lipofermata, and (f) enhanced GLP-1 secretion and exendin[9-39]-inhibitable GSIS in FATP2 inhibitor-treated human islets.

The contribution of glucagon to glucose homeostasis in FATP2KO db/db mice is relatively minor. In the non-fasting, fed state, when β-cells are active, plasma glucagon was decreased in FATP2KO db/db compared to db/db mice, suggesting that glucagon is not the insulin stimulus. To address the glucagon effect more carefully, alanine tolerance tests were conducted in fasting mice, which maximally stimulates glucagon, but not insulin secretion (46). The blunted effect on glucose in FATP2KO db/db compared to db/db mice indicates that some of the glucose-lowering effect of FATP2 deletion could be due to suppressed glucagon-stimulated hepatic gluconeogenesis. While the relatively modest plasma glucose increases in FATP2KO db/db compared to wild-type mice could result in some glucagon-stimulated insulin

release, synthesis of the data from all metabolic studies most strongly support that the predominant FATP2 gene deletion effect on glycemia is the paracrine effect of GLP-1 secretion by α-cells.

Prior investigation of fatty acid effects on GLP-1 secretion is limited. Incubation of a fatty acid mixture with αTC1-6 cells stimulated GLP-1 secretion at low glucose, and suppressed GLP-1 in high glucose conditions (36). Similar results were observed in L-cells, with palmitate inhibition of GLP-1 secretion (47). The stimulation of GLP-1 is primarily by unsaturated fatty acids (36, 48), and is presumed to be mediated by the G-protein coupled FFAR4 in α-cells (49) and FATP4 or FFAR1 in L-cells (48, 50).

FATP2 inhibition was associated with an increased *Pcsk1*:*Pcsk2* mRNA ratio. These data are consistent with palmitate-induced inhibition of islet and L-cell PC1/3 (51-53), which catalyzes the conversion of proglucagon to GLP-1, and proinsulin to insulin (54). Although previous islet studies focused on PC1/3 effects on proinsulin cleavage in β-cells (51-53), it is plausible that FATP2 inhibition also enhances GLP-1 by blocking palmitate-induced PC1/3 suppression in α-cells. Future studies will be required to explore other potential mechanisms of enhanced α-cell GLP-1 secretion, including inhibition of lipotoxicity (36, 47) and reciprocal stimulation of GLP-1 by insulin. While a feed-forward (insulin stimulating GLP-1) mechanism has been proposed for intestinal L-cells (55), similar results in α-cells have not been described.

The insulinotropic effect of GLP-1 on β-cells is due primarily to GLP-1 receptor-mediated augmentation of GSIS. However, sustained hyperinsulinemia in FATP2KO db/db mice was also facilitated by increased β-cell mass and islet hypertrophy, which is a predominately GLP-1-independent process. GLP-1 exerts cytoprotective effects in β-cell lines (56, 57), but in human

285 islets GLP-1 does not stimulate β-cell mitogenesis or affect islet size (57, 58). Identification of
286 the FATP2KO-regulated factors that stimulate islet hypertrophy will require further
287 investigation.

288 The effects of fatty acids on insulin secretion depend on many factors, including fatty
289 acid carbon chain length and saturation, chronicity of exposure, fasting state, and concomitant
290 glucose concentration (16, 59). While palmitate suppressed GLP-1 secretion in αTC1-6 cells, we
291 observed a more modest effect of palmitate on insulin secretion in human islets. However,
292 even in the absence of fatty acids, GSIS was enhanced in Lipofermata-treated islets, suggesting
293 that FATP2 inhibition may mediate insulinotropic effects independent of fatty acid uptake. To
294 date, FATP2 has been linked primarily to lipid metabolism, particularly PPARα-regulated genes
295 (6), which have no effect on pancreatic insulin release (60). Downstream pathways from FATP2
296 are largely unexplored, and identification of additional FATP2-directed events, which may
297 regulate GLP-1-dependent GSIS, are therefore warranted.

298 We conclude that FATP2 deletion or inhibition exerts glucose-lowering effects through
299 α-cell-mediated GLP-1 secretion and paracrine β-cell insulin release. One potential clinical
300 implication is that in contrast to diabetes treatment with GLP-1 receptor agonists, which
301 ostensibly mimic the effect of endogenous GLP-1, FATP2 inhibition may represent a more
302 natural stimulus of α-cell GLP-1 augmentation. Moreover, FATP2 inhibition could represent a
303 potential adjunctive glucose-lowering therapy, and/or a means to delay onset of type 2
304 diabetes.

METHODS

***Sex as a biological variable*.** With the exception of high fat diet experiments, where only male mice develop obesity, no differences were noted between male and female mice for any parameters. Therefore, equal numbers of male and female mice were used in all other experiment.

Mice. Conditional proximal tubule FATP2KO mice were generated from intercrosses between *GGT1*-Cre (JaxLabs) and *Slc27a2*-floxed mice [gift from Dr. Dmitry Gabrilovich (61)] on a congenic C57BL-KS/J background. Genotyping by PCR from toe samples was done by Transnetyx. Type 2 diabetes was induced as previously described (11). Briefly, at six weeks of age, male mice were fed a high fat diet (Harlan, Teklad TD.06414, 60.3% fat, 21.3% carbohydrate, 18.4% protein) for six months. After three months of high fat diet, mice were administered low dose intraperitoneal streptozotocin (45 μg/g) daily for three consecutive days. Diabetes was defined by fasting glucose greater than 200 mg/dL. Glucose and GLP-1 were assayed after fasting from 6:00-10:00 AM. Tail vein blood glucose was assayed by glucometer, as previously described (11).

Immunohistochemistry. Paraffin-embedded human ileum and duodenum slides were purchased from Zyagen. De-paraffinized sections were treated with sodium citrate (10 mM, pH 6.0) for antigen retrieval. Mouse pancreas samples were fixed in paraformaldehyde (4%, 24 hrs, room temp), cryopreserved in sucrose (30% in PBS overnight) and frozen at -80^{o} C. Frozen sections (5 μm by cryostat) were permeabilized with Triton X-100 (Millipore Sigma; 0.2% in PBS, 10 minutes, room temp) and blocked with donkey serum (5% in PBS, 1 hour, room temp). Primary antibodies are listed in Supplemental Table 1. Sections were mounted in SlowFade

Diamond Antifade Mountant with DAPI (Invitrogen) and viewed with a Leica or Olympus confocal microscope.

β-cell and GLP-1-positive α-cell mass. α- and β-cell mass were calculated using published methods (62). Mouse pancreas was fixed in paraformaldehyde (4%, 24 hrs, room temp), weighed, cryopreserved in sucrose (30% in PBS overnight) and frozen at -80^{o} C. Three 5 µm frozen sections, cut 200 µm apart, were analyzed. α- and β-cells were labeled with glucagon and insulin antibodies, respectively, as previously described (11). α- and β-cell areas were normalized to total pancreatic area, and these values were then multiplied by pancreas weight to obtain α- and β-cell mass. GLP-1-positive α-cell mass was determined by multiplying the α-cell mass and the percentage of glucagon-positive cells that co-labeled with GLP-1 antibodies.

Reverse transcriptase polymerase chain reaction (RT-PCR). Methods have previously been described in detail (11). Briefly, total RNA was extracted from whole mouse organs, the mouse αTC1-6 pancreatic α-cell line (ATCC) or the rat INS-1 pancreatic β-cell line (gift from Dr. Yisheng Yang, Case Western Reserve University) using RNeasy Mini Kit (Qiagen). RNA concentrations were determined using the NanoDrop 2000 Spectrophotometer (Thermo Scientific). RT was performed using 5 µg total RNA, and cDNA was generated using SuperScript III First-Strand Synthesis System (Invitrogen). Human α-cell cDNA was purchased from Celprogen. PCR reactions from 1.5 µg cDNA were conducted in 20 µl volume using EmeraldAmp Max PCR Master Mix 2X premix (Takara Bio Inc.), according to recommended protocol and PCR cycling conditions, for 30 cycles (35 cycles for INS-1 cell PCR). Primers were purchased from Eurofins Genomics and sequences are shown in Supplemental Table 2. PCR products underwent 2% agarose gel electrophoresis and bands were identified by ethidium bromide (Invitrogen) staining

and photographed. Quantitative PCR (qPCR) was conducted as previously described (63). Briefly, cDNA was generated using SuperScript III First-Strand, and amplified using the Radiant SYBR Green 2x Master Mix (Alkali Scientific) and QuantStudio 3 System (Applied Biosystems). Quantification was determined by the comparative C_T ($\Delta\Delta C_T$) method.

***FA uptake in αTC1-6 cells*.** Experiments were conducted according to previously described methods (20), using a QBT assay (Molecular Devices). Briefly, αTC1-6 cells (ATCC), which were originally derived from mouse pancreatic α-cells (64), were seeded in 96-well plates, and cultured to confluence over 24 h. Wells were washed with serum-free, phenol-free media for 2 h at 37° C; Lipofermata (5-bromo-5'-phenylspiro[3*H*-1,3,4-thiadiazole-2,3'-indoline]-2-one) (MedChemExpress) was robotically incubated for the final hour. BODIPY-conjugated C18 fatty acids (Molecular Devices QBT assay, 2.5 µM complexed with 0.2 % fatty acid-free albumin carrier + FATP2 inhibitors in QBT loading buffer that contains a proprietary external quenching dye) were robotically added at time = 0. Excitation λ = 490 nm pulses were delivered, and emission λ = 510 nm was recorded at 15-sec intervals for 10 min. BODIPY-labeled fatty acid uptake was determined from fluorescence values obtained at 60 seconds, which is the static time point that most highly correlated with maximum velocity (Supplemental Figure 8). Plates were imaged on the Synergy Neo2 HTX Multi-Mode Microplate reader (BioTek) and averaged from six fields captured from each well using Gen5 software. IC_{50} values were calculated using GraphPad Prism 7 software.

***Hormone assays*.** Glucagon (10-I271-01), GLP-1 (10-I278-01), and human insulin (10-1113-01) were assayed from mouse plasma or culture media by ELISA (Mercodia).

***In vivo metabolic analyses*.** To facilitate multiple blood samples for GLP-1 assays, a carotid artery catheter was placed the day prior to experiments. Mice were fasted for four hours (6:00 AM-10:00 AM) prior to oral (OGTT, 2 g/kg by gavage) or intraperitoneal (IPGTT, 2 g/kg i.p.) glucose tolerance tests (65). Arterial blood was drawn at baseline and then one hr after glucose administration, and plasma was saved at -80^{o} C in tubes containing linagliptin (MedChemExpress; 100 nM) for GLP-1 assays later. Glucometer readings were obtained at baseline, 30, 60, 90 and 120 min. For alanine tolerance tests, fasted mice were administered L-alanine (2 g/kg i.p.), and glucometer readings were obtained at baseline, 10, 30, 45, 60 and 120 min. Non-fasting blood samples for glucagon were obtained in mice by cardiac puncture at the time of sacrifice.

***Glucose-stimulated GLP-1 and insulin secretion*.** Human islets (ProdoLabs) were cultured according to established methods (66). Islets were identified under a dissecting microscope and suspended in RPMI 1640 + 15% FBS for at least 16 hr prior to experimentation. Islets were equilibrated in petri dishes containing modified Krebs buffer (2 mM $NaHCO_3$, 10 mM HEPES, pH 7.4, 37^{o} C, 1 hr). Ten islets were selected and deposited in cell culture wells, with quintuplicate wells for each condition. Initial incubations included modified Krebs buffer supplemented with 2.8 mM glucose (37^{o} C, 1 hr) plus linagliptin (MedChemExpress; 100 nM) ± palmitate (Avanti; 100-400 µM complexed with 0.2% delipidated albumin), Lipofermata (MedChemExpress; 50 µM), or exendin[9-39] (MedChemExpress; 100 nM). After 1 hour, minimum volumes of media for GLP-1 or insulin ELISA assays in duplicate were saved at -80^{o} C. Identical conditions were then repeated for an additional hour in Krebs buffer with high glucose (16.8 mM, 37^{o} C, one hour). Islets were pelleted by centrifugation, lysed in SDS-PAGE buffer, and assayed for protein

content (Nanodrop; absorption at λ = 280 nm). A similar protocol was followed for glucose-stimulated GLP-1 secretion in αTC1-6 cells, except for incubations in 5 mM and 25 mM glucose, to conform with established methods for these cells (37, 38).

Data availability. Data in the manuscript are available in the .xls file within the Supporting data values.

***Statistics*.** Graphical data are presented as mean ± SEM and analyzed using GraphPad Prism 7 software. Data from multiple groups were analyzed by one-way ANOVA and Tukey's post-hoc test for multiple comparisons. Data from two groups were analyzed by unpaired two-tailed *t* test. Statistical significance for all analyses is defined as a *P* value <0.05.

Study approval. All studies were conducted in accordance with protocols approved by the Institutional Animal Care and Use Committee of Case Western Reserve University School of Medicine.

ACKNOWLEDGMENTS

The authors thank Hanxiao Liu and Dr. Yan Li, CWRU Dept of Genetics, for assistance with islet selection and culture methods.

Funding: This work is the result of NIH funding (5R01DK064819 to DA, 2R01DK067528 to JRS), in whole or in part, and is subject to the NIH Public Access Policy. Through acceptance of this federal funding, the NIH has been given a right to make the work publicly available in PubMed Central.

Author contributions: SK, RJG, ZL, VL conducted experiments, acquired data, analyzed data, and reviewed/edited the manuscript; IS, contributed reagents, contributed to discussion and reviewed/edited the manuscript; JS contributed to discussion and reviewed/edited the manuscript; PO-O conducted experiments, acquired data and reviewed/edited the manuscript; JLG conducted experiments, analyzed data, and reviewed/edited the manuscript; DA designed research studies, analyzed data and reviewed/edited the manuscript; JRS obtained funding, designed research studies, analyzed data, wrote and edited the manuscript.

REFERENCES

1. Reidy K, Kang HM, Hostetter T, and Susztak K. Molecular mechanisms of diabetic kidney disease. *J Clin Invest.* 2014;124(6):2333-40.
2. Eid S, Sas KM, Abcouwer SF, Feldman EL, Gardner TW, Pennathur S, et al. New insights into the mechanisms of diabetic complications: role of lipids and lipid metabolism. *Diabetologia.* 2019;62(9):1539-49.
3. Sobczak AIS, Blindauer CA, and Stewart AJ. Changes in plasma free fatty acids associated with type-2 diabetes. *Nutrients.* 2019;11(9).
4. Hirsch D, Stahl A, and Lodish HF. A family of fatty acid transporters conserved from mycobacterium to man. *Proc Natl Acad Sci USA.* 1998;95(15):8625-9.
5. Qiu P, Wang H, Zhang M, Zhang M, Peng R, Zhao Q, et al. FATP2-targeted therapies - A role beyond fatty liver disease. *Pharmacol Res.* 2020;161:105228.
6. Perez VM, Gabell J, Behrens M, Wase N, DiRusso CC, and Black PN. Deletion of Fatty Acid Transport Protein 2 (FATP2) in the mouse liver changes the metabolic landscape by increasing the expression of PPARα-regulated genes. *J Biol Chem.* 2020;295(17):5737-50.
7. Falcon A, Doege H, Fluitt A, Tsang B, Watson N, Kay MA, et al. FATP2 is a hepatic fatty acid transporter and peroxisomal very long-chain acyl-CoA synthetase. *Am J Physiol Endocrinol Metab.* 2010;299(3):E384-93.
8. Lewis DL, and Wolff JA. Delivery of siRNA and siRNA expression constructs to adult mammals by hydrodynamic intravascular injection. *Methods Enzymol.* 2005;392:336-50.
9. Bradley SP, Rastellini C, da Costa MA, Kowalik TF, Bloomenthal AB, Brown M, et al. Gene silencing in the endocrine pancreas mediated by short-interfering RNA. *Pancreas.* 2005;31(4):373-9.
10. Larson SD, Jackson LN, Chen LA, Rychahou PG, and Evers BM. Effectiveness of siRNA uptake in target tissues by various delivery methods. *Surgery.* 2007;142(2):262-9.
11. Khan S, Gaivin RJ, Abramovich C, Boylan M, Calles J, and Schelling JR. Fatty acid transport protein-2 (FATP2) regulates glycemic control and diabetic kidney disease progression. *JCI insight.* 2020;5(15):136845.
12. Holter MM, Saikia M, and Cummings BP. Alpha-cell paracrine signaling in the regulation of beta-cell insulin secretion. *Front Endocrinol* 2022;13:934775.
13. Jorsal T, Rhee NA, Pedersen J, Wahlgren CD, Mortensen B, Jepsen SL, et al. Enteroendocrine K and L cells in healthy and type 2 diabetic individuals. *Diabetologia.* 2018;61(2):284-94.
14. Mancini AD, and Poitout V. The fatty acid receptor FFA1/GPR40 a decade later: how much do we know? *Trends Endocrinol Metab.* 2013;24(8):398-407.
15. Campbell JE, and Newgard CB. Mechanisms controlling pancreatic islet cell function in insulin secretion. *Nat Rev Mol Cell Biol.* 2021;22(2):142-58.
16. Haber EP, Procópio J, Carvalho CR, Carpinelli AR, Newsholme P, and Curi R. New insights into fatty acid modulation of pancreatic beta-cell function. *Int Rev Cytol.* 2006;248:1-41.
17. Marchetti P, Lupi R, Bugliani M, Kirkpatrick CL, Sebastiani G, Grieco FA, et al. A local glucagon-like peptide 1 (GLP-1) system in human pancreatic islets. *Diabetologia.* 2012;55(12):3262-72.
18. Ellingsgaard H, Hauselmann I, Schuler B, Habib AM, Baggio LL, Meier DT, et al. Interleukin-6 enhances insulin secretion by increasing glucagon-like peptide-1 secretion from L cells and alpha cells. *Nat Med.* 2011;17(11):1481-9.
19. Kieffer TJ, McIntosh CH, and Pederson RA. Degradation of glucose-dependent insulinotropic polypeptide and truncated glucagon-like peptide 1 in vitro and in vivo by dipeptidyl peptidase IV. *Endocrinology.* 1995;136(8):3585-96.

20. Khan S, Cabral PD, Schilling WP, Schmidt ZW, Uddin AN, Gingras A, et al. Kidney proximal tubule lipoapoptosis is regulated by Fatty Acid Transporter-2 (FATP2). *J Am Soc Nephrol.* 2018;29(1):81-91.
21. Park J, Shrestha R, Qiu C, Kondo A, Huang S, Werth M, et al. Single-cell transcriptomics of the mouse kidney reveals potential cellular targets of kidney disease. *Science.* 2018;360(6390):758-63.
22. Gerich JE. Role of the kidney in normal glucose homeostasis and in the hyperglycaemia of diabetes mellitus: therapeutic implications. *Diabet Med.* 2010;27(2):136-42.
23. Schrimpe-Rutledge AC, Fontes G, Gritsenko MA, Norbeck AD, Anderson DJ, Waters KM, et al. Discovery of novel glucose-regulated proteins in isolated human pancreatic islets using LC-MS/MS-based proteomics. *J Proteome Res.* 2012;11(7):3520-32.
24. Dalbøge LS, Almholt DL, Neerup TS, Vassiliadis E, Vrang N, Pedersen L, et al. Characterisation of age-dependent beta cell dynamics in the male db/db mice. *PLoS One.* 2013;8(12):e82813.
25. Adriaenssens AE, Svendsen B, Lam BY, Yeo GS, Holst JJ, Reimann F, et al. Transcriptomic profiling of pancreatic α, ß and δ cell populations identifies δ cells as a principal target for ghrelin in mouse islets. *Diabetologia.* 2016;59(10):2156-65.
26. Muraro MJ, Dharmadhikari G, Grün D, Groen N, Dielen T, Jansen E, et al. A single-cell transcriptome atlas of the human pancreas. *Cell Syst.* 2016;3(4):385-94.e3.
27. Segerstolpe Å, Palasantza A, Eliasson P, Andersson EM, Andréasson AC, Sun X, et al. Single-cell transcriptome profiling of human pancreatic islets in health and type 2 diabetes. *Cell Metab.* 2016;24(4):593-607.
28. Tarifeño-Saldivia E, Lavergne A, Bernard A, Padamata K, Bergemann D, Voz ML, et al. Transcriptome analysis of pancreatic cells across distant species highlights novel important regulator genes. *BMC Biol.* 2017;15(1):21.
29. Oropeza D, Cigliola V, Romero A, Chera S, Rodríguez-Seguí SA, and Herrera PL. Stage-specific transcriptomic changes in pancreatic α-cells after massive β-cell loss. *BMC Genomics.* 2021;22(1):585.
30. Sturgill D, Wang L, and Arda HE. PancrESS - a meta-analysis resource for understanding cell-type specific expression in the human pancreas. *BMC Genomics.* 2024;25(1):76.
31. Melton EM, Cerny RL, Watkins PA, DiRusso CC, and Black PN. Human fatty acid transport protein 2a/very long chain acyl-CoA synthetase 1 (FATP2a/Acsvl1) has a preference in mediating the channeling of exogenous n-3 fatty acids into phosphatidylinositol. *J Biol Chem.* 2011;286(35):30670-9.
32. Ahowesso C, Black PN, Saini N, Montefusco D, Chekal J, Malosh C, et al. Chemical inhibition of fatty acid absorption and cellular uptake limits lipotoxic cell death. *Biochem Pharmacol.* 2015;98(1):167-81.
33. Kumar M, Gaivin RJ, Khan S, Fedorov Y, Adams DJ, Zhao W, et al. Definition of fatty acid transport protein-2 (FATP2) structure facilitates identification of small molecule inhibitors for the treatment of diabetic complications. *Int J Biol Macromol.* 2023:125328.
34. Weir GC, and Bonner-Weir S. Conflicting views about interactions between pancreatic α-cells and β-cells. *Diabetes.* 2023;72(12):1741-7.
35. Small L, Ehrlich A, Iversen J, Ashcroft SP, Trošt K, Moritz T, et al. Comparative analysis of oral and intraperitoneal glucose tolerance tests in mice. *Mol Metab.* 2022;57:101440.
36. Sancho V, Daniele G, Lucchesi D, Lupi R, Ciccarone A, Penno G, et al. Metabolic regulation of GLP-1 and PC1/3 in pancreatic α-cell line. *PLoS One.* 2017;12(11):e0187836.
37. Whalley NM, Pritchard LE, Smith DM, and White A. Processing of proglucagon to GLP-1 in pancreatic α-cells: is this a paracrine mechanism enabling GLP-1 to act on ß-cells? *J Endocrinol.* 2011;211(1):99-106.

38. Piro S, Mascali LG, Urbano F, Filippello A, Malaguarnera R, Calanna S, et al. Chronic exposure to GLP-1 increases GLP-1 synthesis and release in a pancreatic alpha cell line (α-TC1): evidence of a direct effect of GLP-1 on pancreatic alpha cells. *PLoS One.* 2014;9(2):e90093.
39. Traub S, Meier DT, Schulze F, Dror E, Nordmann TM, Goetz N, et al. Pancreatic α cell-derived glucagon-related peptides are required for β cell adaptation and glucose homeostasis. *Cell Rep.* 2017;18(13):3192-203.
40. Kilimnik G, Kim A, Steiner DF, Friedman TC, and Hara M. Intraislet production of GLP-1 by activation of prohormone convertase 1/3 in pancreatic alpha-cells in mouse models of ss-cell regeneration. *Islets.* 2010;2(3):149-55.
41. O'Malley TJ, Fava GE, Zhang Y, Fonseca VA, and Wu H. Progressive change of intra-islet GLP-1 production during diabetes development. *Diabetes Metab Res Rev.* 2014;30(8):661-8.
42. Hansen AM, Bodvarsdottir TB, Nordestgaard DN, Heller RS, Gotfredsen CF, Maedler K, et al. Upregulation of alpha cell glucagon-like peptide 1 (GLP-1) in Psammomys obesus--an adaptive response to hyperglycaemia? *Diabetologia.* 2011;54(6):1379-87.
43. Talchai C, Xuan S, Lin HV, Sussel L, and Accili D. Pancreatic β cell dedifferentiation as a mechanism of diabetic β cell failure. *Cell.* 2012;150(6):1223-34.
44. Wideman RD, Yu IL, Webber TD, Verchere CB, Johnson JD, Cheung AT, et al. Improving function and survival of pancreatic islets by endogenous production of glucagon-like peptide 1 (GLP-1). *Proc Natl Acad Sci U S A.* 2006;103(36):13468-73.
45. Kanoski SE, Hayes MR, and Skibicka KP. GLP-1 and weight loss: unraveling the diverse neural circuitry. *Am J Physiol Regul Integr Comp Physiol.* 2016;310(10):R885-95.
46. Capozzi ME, Wait JB, Koech J, Gordon AN, Coch RW, Svendsen B, et al. Glucagon lowers glycemia when β-cells are active. *JCI insight.* 2019;5(16).
47. Filippello A, Urbano F, Di Mauro S, Scamporrino A, Di Pino A, Scicali R, et al. Chronic exposure to palmitate impairs insulin signaling in an intestinal L-cell Line: A possible shift from GLP-1 to glucagon production. *Int J Mol Sci.* 2018;19(12):3791.
48. Thombare K, Ntika S, Wang X, and Krizhanovskii C. Long chain saturated and unsaturated fatty acids exert opposing effects on viability and function of GLP-1-producing cells: Mechanisms of lipotoxicity. *PLoS One.* 2017;12(5):e0177605.
49. Campbell SA, Johnson J, and Light PE. Evidence for the existence and potential roles of intra-islet glucagon-like peptide-1. *Islets.* 2021;13(1-2):32-50.
50. Poreba MA, Dong CX, Li SK, Stahl A, Miner JH, and Brubaker PL. Role of fatty acid transport protein 4 in oleic acid-induced glucagon-like peptide-1 secretion from murine intestinal L cells. *Am J Physiol Endocrinol Metab.* 2012;303(7):E899-907.
51. Wen Q, Chowdhury AI, Aydin B, Shekha M, Stenlid R, Forslund A, et al. Metformin restores prohormone processing enzymes and normalizes aberrations in secretion of proinsulin and insulin in palmitate-exposed human islets. *Diabetes Obes Metab.* 2023;25(12):3757-65.
52. Iida H, Kono T, Lee CC, Krishnan P, Arvin MC, Weaver SA, et al. SERCA2 regulates proinsulin processing and processing enzyme maturation in pancreatic beta cells. *Diabetologia.* 2023;66(11):2042-61.
53. Hayashi H, Yamada R, Das SS, Sato T, Takahashi A, Hiratsuka M, et al. Glucagon-like peptide-1 production in the GLUTag cell line is impaired by free fatty acids via endoplasmic reticulum stress. *Metabolism.* 2014;63(6):800-11.
54. Ramzy A, Asadi A, and Kieffer TJ. Revisiting proinsulin processing: Evidence that human β-cells process proinsulin with prohormone convertase (PC) 1/3 but not PC2. *Diabetes.* 2020;69(7):1451-62.

55. Yi F, Sun J, Lim GE, Fantus IG, Brubaker PL, and Jin T. Cross talk between the insulin and Wnt signaling pathways: evidence from intestinal endocrine L cells. *Endocrinology.* 2008;149(5):2341-51.
56. Cornu M, Yang JY, Jaccard E, Poussin C, Widmann C, and Thorens B. Glucagon-like peptide-1 protects beta-cells against apoptosis by increasing the activity of an IGF-2/IGF-1 receptor autocrine loop. *Diabetes.* 2009;58(8):1816-25.
57. Drucker DJ. Incretin action in the pancreas: potential promise, possible perils, and pathological pitfalls. *Diabetes.* 2013;62(10):3316-23.
58. Rosselot C, Li Y, Wang P, Alvarsson A, Beliard K, Lu G, et al. Harmine and exendin-4 combination therapy safely expands human β cell mass in vivo in a mouse xenograft system. *Sci Transl Med.* 2024;16(755):eadg3456.
59. Prentki M, Matschinsky FM, and Madiraju SR. Metabolic signaling in fuel-induced insulin secretion. *Cell Metab.* 2013;18(2):162-85.
60. Guerre-Millo M, Rouault C, Poulain P, André J, Poitout V, Peters JM, et al. PPAR-alpha-null mice are protected from high-fat diet-induced insulin resistance. *Diabetes.* 2001;50(12):2809-14.
61. Veglia F, Tyurin VA, Blasi M, De Leo A, Kossenkov AV, Donthireddy L, et al. Fatty acid transport protein 2 reprograms neutrophils in cancer. *Nature.* 2019;569(7754):73-8.
62. Bru-Tari E, Cobo-Vuilleumier N, Alonso-Magdalena P, Dos Santos RS, Marroqui L, Nadal A, et al. Pancreatic alpha-cell mass in the early-onset and advanced stage of a mouse model of experimental autoimmune diabetes. *Sci Rep.* 2019;9(1):9515.
63. Lakhe-Reddy S, Khan S, Konieczkowski M, Jarad G, Wu KL, Reichardt LF, et al. ß8 integrin binds Rho GDP dissociation inhibitor-1 and activates Rac1 to inhibit mesangial cell myofibroblast differentiation. *J Biol Chem.* 2006;281(28):19688-99.
64. Powers AC, Efrat S, Mojsov S, Spector D, Habener JF, and Hanahan D. Proglucagon processing similar to normal islets in pancreatic alpha-like cell line derived from transgenic mouse tumor. *Diabetes.* 1990;39(4):406-14.
65. Al Rijjal D, and Wheeler MB. A protocol for studying glucose homeostasis and islet function in mice. *STAR Protoc.* 2022;3(1):101171.
66. Son J, Du W, Esposito M, Shariati K, Ding H, Kang Y, et al. Genetic and pharmacologic inhibition of ALDH1A3 as a treatment of β-cell failure. *Nat Commun.* 2023;14(1):558.

588

589 **Figure 1. Islet hypertrophy and increased β-cell mass in FATP2KO db/db mice.** Representative
590 immunohistochemistry images of pancreatic islets from db/db (**A**) and FATP2KO db/db (**B**) mice.
591 α- and β-cells were labeled with glucagon and insulin antibodies, respectively, as described in
592 Methods. (**C**) β-cell mass was calculated as described in Methods for db/db and FATP2KO db/db
593 mice. *P <0.01 by Student's t-test.

594 **Figure 2. FATP2 expression localizes to pancreatic α-cells in mouse islets.** Wild-type mouse
595 pancreas islets were immunohistochemically labeled for FATP2 expression in α-, β- and δ-cells
596 as described in Methods. Merged images, representing cell-specific FATP2 expression are shown
597 in yellow. Micrometer scale bars are shown at the bottom right of each merged image.

598 **Figure 3. FATP2 expression localizes to pancreatic α-cells in human islets.** (**A**) Paraffin sections
599 of human pancreas were immunohistochemically labeled for FATP2 expression in α- and β-cells
600 as described in Methods. Merged images, representing cell-specific FATP2 expression are shown
601 in yellow. Micrometer scale bars are shown at the bottom of each image. (**B**) Gene expression
602 correlation between preproglucagon (GCG) and FATP2 (SLC27A2) from two public normal
603 human islet transcriptome datasets (GSE38642 and GSE50397) using online software
604 (http://r2.amc.nl). Data were analyzed by linear regression and Pearson correlation.

605 **Figure 4. FATP2 expression and function in α-cells.** (**A** and **B**) FATP2 and loading control GAPDH
606 mRNA expression were determined in human and mouse pancreatic tissue and α-cell lines by
607 RT-PCR (as described in Methods). Data are representative of three experiments per condition.
608 (**C**) Mouse αTC1-6 cells were pre-incubated with Lipofermata (1 hr, 37° C, 0–50 μM) in triplicate.

609 BODIPY-labeled fatty acid uptake velocity was then determined, as described in Methods.
610 Results are mean ± SEM from four experiments.

611 **Figure 5. Effects of FATP2 deletion on glucagon.** (**A**) Random (non-fasting) plasma glucagon
612 concentrations in four to six months old wild-type and db/db mice ± FATP2 gene deletion. Each
613 symbol in the scatter bars represents mean from one sample assayed in duplicate. Therefore, N
614 = glucagon concentrations from 9-17 mice per genotype. *P <0.05 compared to wild-type by
615 ANOVA with Tukey's post-hoc test for multiple comparisons. (**B**) Serial glucose measurements in
616 four to six month old wild-type and db/db mice ± FATP2 gene deletion (N = 3 mice per group)
617 following alanine administration (2 g/kg i.p.).

618 **Figure 6. Blood glucose and plasma GLP-1 concentrations following oral (OGTT) and**
619 **intraperitoneal (IPGTT) glucose tolerance tests.** (**A**) OGTT and IPGTT were conducted in db/db
620 and FATP2KO db/db mice, as described in Methods. Blood glucose was determined at the
621 indicated times in five mice per group. (**B**) As an index of glucose disposal, the area under the
622 curve (AUC) corresponding to FATP2KO db/db experiments in (**A**) was integrated using GraphPad
623 Prism 7 software. (**C**) Plasma was obtained at baseline and at the one hr time point during OGTT
624 or IPTGG in FATP2KO db/db mice.

625 **Figure 7. FATP2 and GLP-1 localization in intestine.** FATP2 (**A**) and preproglucagon (**B**) mRNA
626 expression were determined in mouse gut segments by qPCR, as described in Methods. Data
627 are normalized to stomach expression, which is defined as 1.0. Immunohistochemical labeling
628 of FATP2 and GLP-1 in human distal ileum (**C** and **D**, note that FATP2 is red and GLP-1 is green)
629 and duodenum (**E** and **F**, note that FATP2 is green and GLP-1 is red) are representative from five
630 mice.

Figure 8. FATP2KO/deletion effect on glucose-stimulated GLP-1 and insulin secretion. (**A**) Pancreas GLP-1-positive α-cell mass was determined as described in Methods in db/db and FATP2KO db/db mice. * P <0.01 compared to db/db group by t-test. (**B**) Human islets were pre-incubated with or without Lipofermata (LF), then tested for glucose-stimulated GLP-1 secretion as described in Methods. * P <0.01 compared to all other groups by ANOVA. (**C**) αTC1-6 cells were pre-incubated with or without Lipofermata (LF) or palmitate (Palm) as indicated. Glucose-stimulated GLP-1 secretion was then measured as described in Methods. Each symbol in the B and C scatter bars represents one sample that was assayed in duplicate. Therefore, N = 3-6 samples per condition. * P <0.05 compared LF + Palm by ANOVA. (**D**) αTC1-6 cells co-incubated in 5 mM or 25 mM glucose ± 400 µM palmitate (Palm) ± 50 µM Lipofermata (LF) for 16 hrs were analyzed for *Pcsk1* and *Pcsk2* mRNA expression by qPCR, and expressed as the ratio relative to 5 mM glucose only condition. *P <0.05 compared to other groups by ANOVA. (**E**) Glucose-stimulated insulin secretion was measured in human islets, which were pre-incubated with Lipofermata (LF) and then exposed to exendin[9-39] (Ex) or palmitate (Palm), as described in Methods. Each symbol in the scatter bars represents one sample that was assayed in duplicate. Therefore, N = 3 samples per condition. * P <0.01 compared to 16.8 mM glucose + LF group by ANOVA.

649 Figure 1

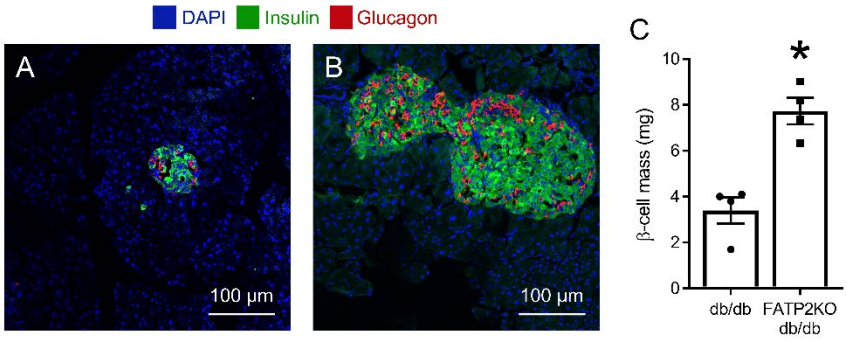

650

651 Figure 2

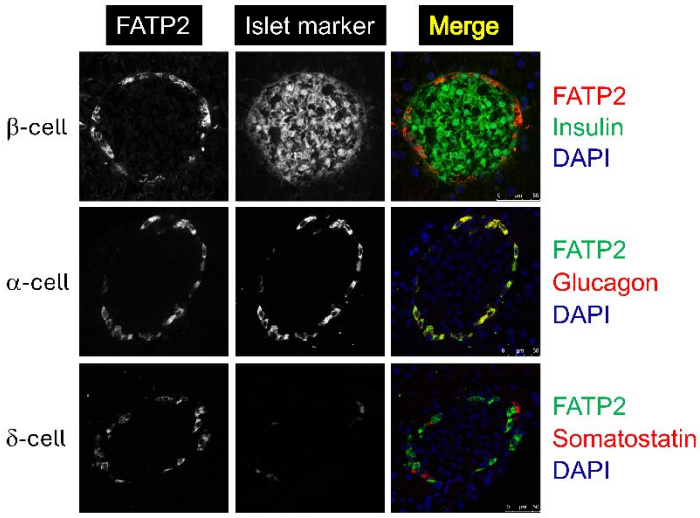

652

653 Figure 3

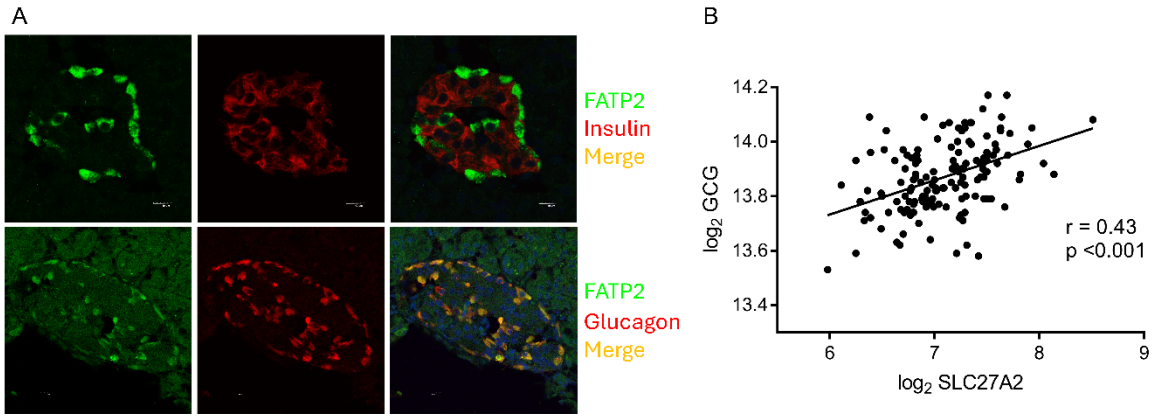

654

655 Figure 4

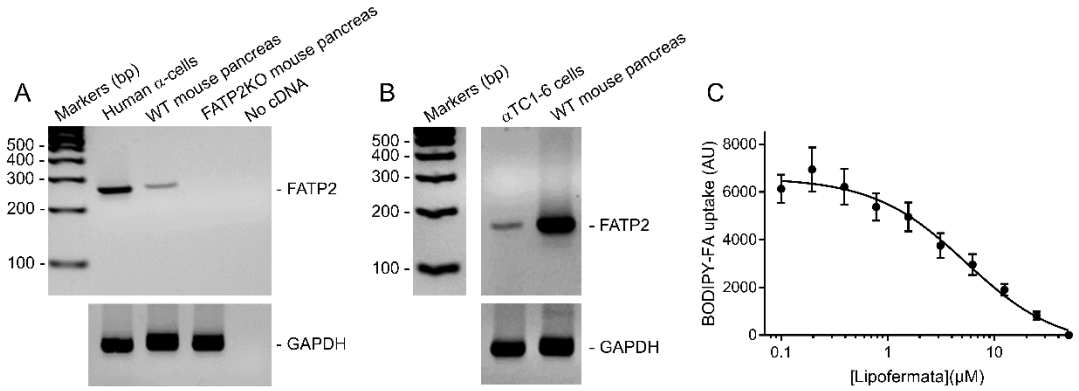

656

657 Figure 5

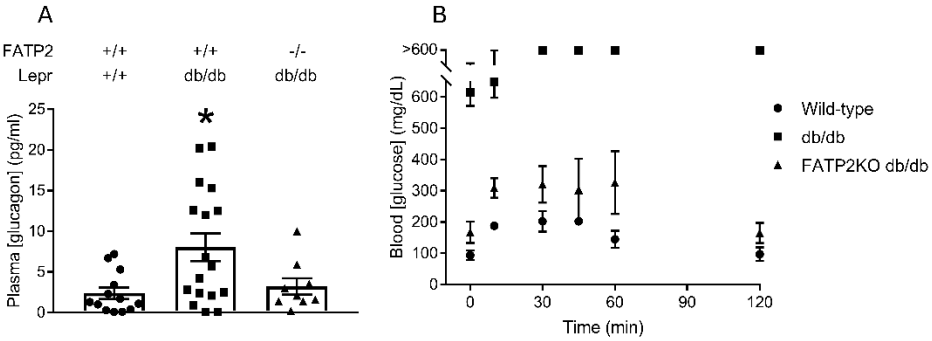

658

659 Figure 6

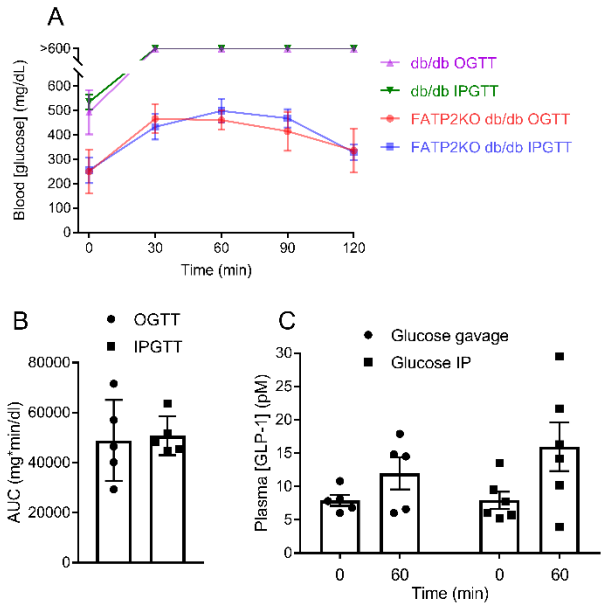

660

661 Figure 7

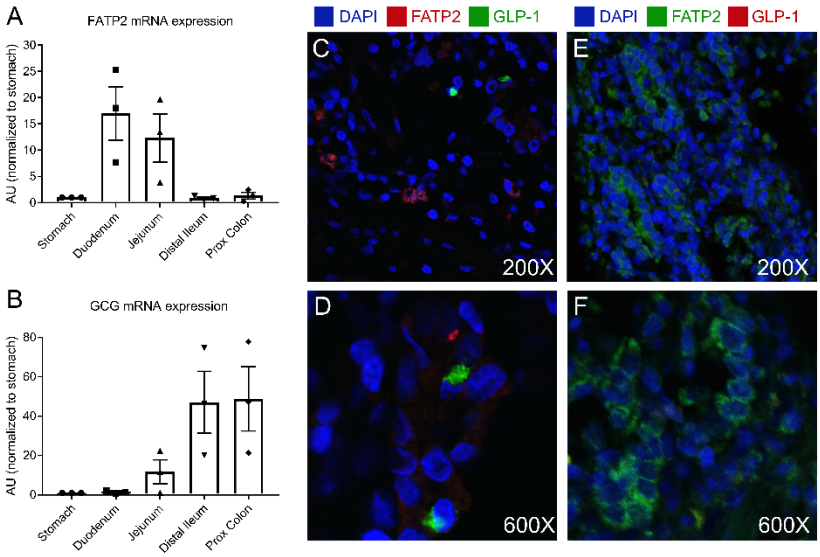

662

663 Figure 8

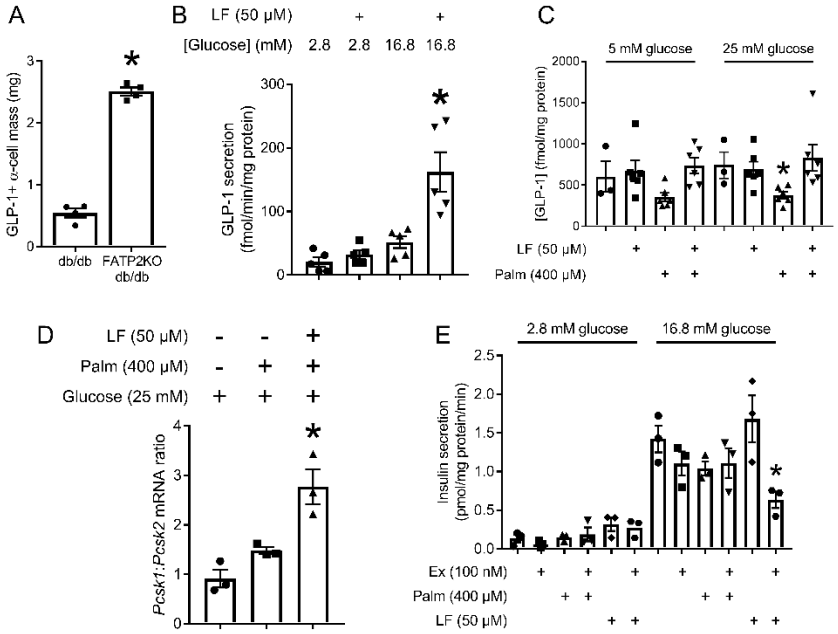

664